Synthesis and Preferred All-*syn* Conformation of C_3-Symmetrical *N*-(Hetero)arylmethyl Triindoles

Eva M. García-Frutos,[a] Berta Gómez-Lor,*[a] Ángeles Monge,[a] Enrique Gutiérrez-Puebla,[a] Ibon Alkorta,[b] and José Elguero[b]

Abstract: A new series of C_3-symmetrical *N*-(hetero)arylmethyl triindoles has been synthesized in a straightforward procedure. The structure and conformation in the solid state have been determined for three derivatives (**3**, **4**, and **6**) by X-ray crystallographic analysis. In all three cases, the molecules adopt a tripodal conformation with all of the flexible arms directed towards the same side, thereby delimiting an inner cavity. Compound **6** crystallizes and forms C_3-symmetric dimeric cage-like complexes. Guest molecules of chloroform and water are confined within the resulting cavities with stabilization by different intermolecular interactions; this highlights the potential of these compounds in the construction of supramolecular systems. A computational analysis has been performed to predict the most stable conformers. As a general trend, a preference for a conformation with all branches directed to the same side has been predicted. Comparison between theoretical and experimental results indicates that the computational level selected for the present study, B3LYP/6-31G*, is able to reproduce both the minimum energy conformations and the rotation barriers about the N—CH₂ bond.

Introduction

Tripodal molecular scaffolds with different degrees of cavity preorganization have long been envisaged as attractive motifs in supramolecular chemistry[1] to create, among other things, synthetic receptors, metal-encapsulating ligands, molecular switches, or sensing devices.

Numerous supramolecular systems have been constructed based on rigid platforms, which primarily determine the shape, and flexibly attached pendant groups; these systems have a thermodynamically favored tripodal conformation that is determined by the chemical nature of the backbone and pendant groups. By exploiting this concept of conformer discrimination by thermodynamically favored preorganization, a great number of tripodal persubstituted benzene-based supramolecular hosts for small- and medium-sized guests have been synthesized.[2,3] Comparably few examples have been reported with extended aromatic cores to target bigger, more complex structures.[4]

Herein, we wish to report the syntheses and conformation studies for *N*-(hetero)arylmethyl derivatives of heptacyclic 10,15-dihydro-5*H*-diindolo[3,2-*a*:3′,2′-*c*]carbazole (triindole), a C_3-symmetric molecule that can be considered as an extended π system in which three carbazole units share a central aromatic ring. Curiously, whereas its all-carbon counterpart, truxene, has been recognized as a potential starting material for the construction of fullerene fragments,[5] C_3 tripodal materials,[6] electrooptical devices,[7] and liquid–crystalline compounds,[8] triindole derivatives have only recently been explored,[9] probably due to the lack of a general, versatile synthetic access to this molecule. We have recently reported a convenient synthesis of **1** from a known symmetrical hexabromotriindole[10] by palladium-catalyzed reductive debromination with triethylammonium formate; this allows for the preparation of **1** on a large scale.[11] With the aim of developing systems for the construction of C_3 tripods based on the triindole platform **1**, we have studied and are reporting herein the alkylation of this electron-rich molecule. Theoretical investigations predict a preference for an all-*syn* conformation for these derivatives. Additionally, X-ray anal-

[a] Dr. E. M. García-Frutos, Dr. B. Gómez-Lor, Prof. Dr. Á. Monge, Prof. Dr. E. Gutiérrez-Puebla
Instituto de Ciencia de Materiales de Madrid, CSIC
Cantoblanco, 28049 Madrid (Spain)
Fax: (+34) 91-3349031
E-mail: bgl@icmm.csic.es

[b] Prof. Dr. I. Alkorta, Prof. Dr. J. Elguero
Instituto de Química Médica, CSIC
Juan de la Cierva 3, 28006 Madrid (Spain)

ysis confirms that this is the favored conformation in the solid state.

Results and Discussion

Synthesis: The synthesis of **2–9** (Scheme 1) was achieved by alkylation of **1** under phase-transfer conditions. Thus, treatment of **1** with the corresponding alkyl halides in the presence of KOH as a base and tetrabutylammonium hydrogen sulfate as a solid–liquid phase-transfer catalyst in acetone under reflux conditions yielded the tris-alkylated triindoles **2–9** in good yields.
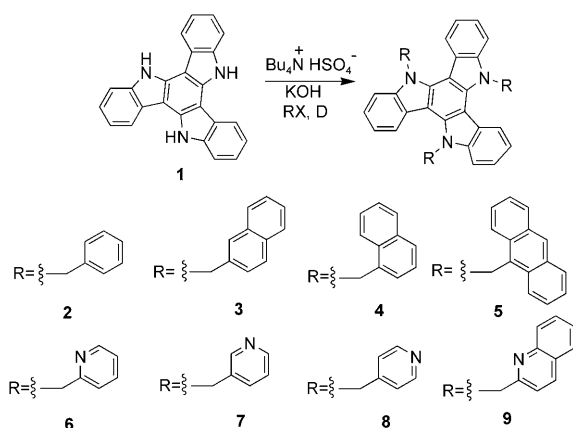
Scheme 1. Synthesis of the *N*-substituted triindoles **2–9**.

Static aspects: X-ray crystallography: Crystals of compounds **3**, **4**, and **6** suitable for single-crystal X-ray analysis were obtained from slow evaporation of tetrachloroethane (for **3**) or chloroform solutions (for **4** and **6**; Figure 1). Compounds **3** and **6** recrystallize in a trigonal system, whereas compound **4** recrystallizes in a monoclinic one.

X-ray structure analysis revealed that the triindole platforms are slightly twisted, with the three peripheral rings bending (≈8°) out of the plane of the central ring, all toward the same side. In all cases, the *N*-(hetero)aryl branches are placed above and nearly orthogonal to the triindole platform in an all-*syn* conformation (*u,u,u*)[12] with the CH₂ groups below the triindole platform (*B,B,B*).[12] In all three molecules, a cavity is formed (Figure 1) by the three (hetero)aryl groups. In compound **6**, the nitrogen atoms of the pyridyl moieties adopt an *exo* arrangement with respect to the inner cavity (*out*).[12]

The molecular packing of the naphthyl derivatives **3** and **4** in the crystal is characterized by a face-to-face arrangement of the triindole units, which are placed with a distance of 3.64 Å between the centroids of the central benzene rings. In the crystal packing, each naphthalene branch on the triindole base interacts with two naphthalene units of two different adjacent molecules; this gives rise to short intermolecular contacts.
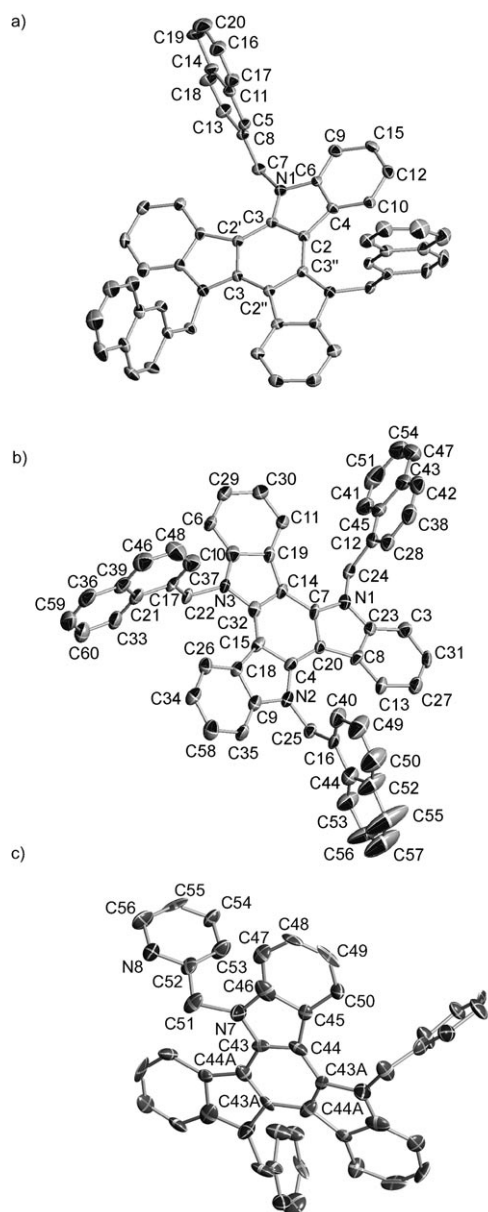

Figure 1. ORTEP plots for a) **3**, b) **4** and c) one crystallographically independent molecule of **6**.

The unit cell of **6** consists of six molecules forming three crystallographically independent C_3-symmetric dimeric aggregates (average distance between the centroids of the central aromatic rings of the platforms is 7.25 Å), one of them encaging a molecule of water and the others housing chloroform (Figure 2).

The water-housing dimers are composed of two equal enantiomers facing each other with the pyridyl substituents in an alternate arrangement (Figure 2a). A molecular unit is rotated 60° with respect to the next one, so the central aromatic rings of the triindole platforms are perfectly superimposable. One positionally disordered water molecule is encaged in each of these dimers. By contrast, the chloroform-housing dimeric cages are formed by two different enantio-
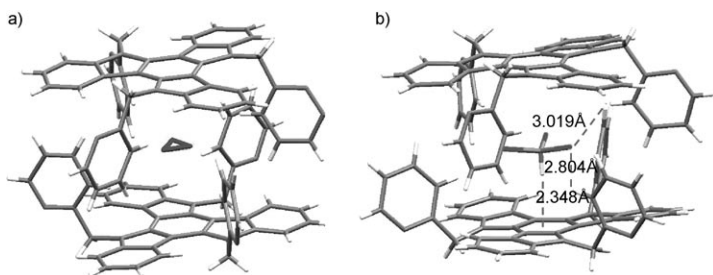
Figure 2. a) View of the **6**₂·H₂O complex, which shows an H₂O molecule disordered in three different positions. b) View of one of the **6**₂·CHCl₃ complexes, which shows the CHCl₃ molecule and the intermolecular interactions between the chloroform molecule and the triindole cage. The complex has C_{3v} symmetry, so only one third of the interactions are represented.

mers, with the pyridyl moieties mutually facing each other and with each molecule rotated 30° with respect to the next molecular unit (Figure 2b). The molecule of chloroform is placed within the cavity with the carbon and hydrogen atoms located on the C_3 axis. The hydrogen atom in the chloroform molecule points toward one of the triindole platforms, establishing a CH/π interaction with the central benzene ring, while the chlorine atoms form nonconventional C−H···Cl hydrogen bonds with the three inward hydrogen atoms of the pyridyl branches. Short contacts between the chlorine atoms and the three inward hydrogen atoms of the pyridyl branches of the opposite molecular unit are also observed (Figure 2b).

Cages of the same class form columns by stacking along the crystallographic *c* axis. In the stacks, the dimeric complexes encaging a molecule of water are at an average distance of 3.45 Å (centroid–centroid distance between the central benzene rings of the platforms). Columns formed by cages housing a water molecule are surrounded by six columns of dimers encaging chloroform (Figure 3).

Dynamic aspects: NMR study: The ¹H NMR spectra of **2**–**9** show single sets of resonances that are indicative of time-averaged C_3 symmetry in solution. The two methylene pro-
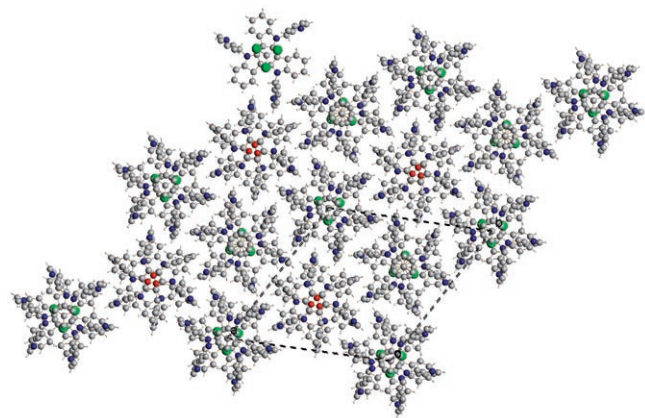

Figure 3. Packing of **6** along the *c* axis.

tons on the arylmethyl substituents are magnetically equivalent, which suggests rapid rotation of the three branches about the C−N bonds on the NMR timescale. To gain insight into this dynamic process and to assess conformation preferences, variable-temperature ¹H NMR experiments in CD₂Cl₂ were performed.

The signals of the methylene protons on the arylmethyl substituents gradually broaden upon cooling; this reflects a progressive freezing of the side arms. By using the chemical shifts, *ν*, of diastereotopic protons H_a and H_b of the N−CH₂ group (which, upon a decrease in the temperature, move from an A₂ towards an AB system), a geminal coupling constant of $J_{AB} = -14$ Hz (from an *N*-benzyl heterocycle),[13] and the fact that, at the coalescence temperature, the rate of rotation $k = \pi/\sqrt{2}[(\nu_A - \nu_B)^2 + 6J_{AB}^2]^{1/2}$ and the rotation barrier at temperature T $\Delta G_{\ddagger}^T = 19.12\,T(10.32 + \lg T/k)$ (in kJ mol⁻¹), we have obtained the data in Table 1.

Table 1. Estimation of the rotation barriers of *N*-(hetero)arylmethyl triindoles from the ¹H NMR spectra at 500 MHz.

Compound	$T_{coalescence}$ [K]	$\nu_A - \nu_B$ [ppm, Hz]	$\Delta G_{\ddagger}^T$ [kJ mol⁻¹]
3	≈195	1.256, 628	35.3
6	≈187	1.0895, 545	34.0
7	≈180	0.873, 436	33.0
8	≈200	1.068, 534	36.5
9	≈200	1.132, 566	36.4
average			35.0

The low precision in the estimation of the temperature of coalescence prevents discussion of individual values; the main conclusion is that these compounds show rotation barriers of about (35±2) kJ mol⁻¹. These barriers correspond to a triple *u,u,u/d,d,d*[12] rotation (Scheme 2), the only one that is able to exchange the H_a and H_b protons of the CH₂−Ar-(Het) groups. There is only one series of signals for the three CH₂ groups on the NMR timescale because the three inversion processes take place simultaneously. The nitrogen inversion does not affect the observed coalescence.

Figure 4 shows the experimental ¹H NMR methylene proton signals of compound **6** between 178 and 298 K and the simulated spectra obtained with different rate constants. The simulations were generated by using the gNMR program.[14] Even at the lowest temperature reached (178 K), the AB pattern is not observed, but a coupling of −14 Hz is necessary to reproduce the spectra. By eliminating the two highest temperature values (273 and 298 K) for being too
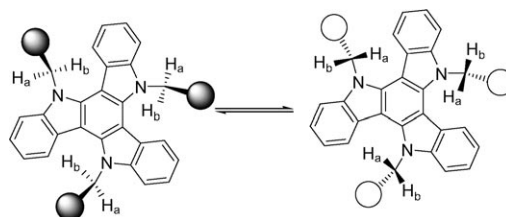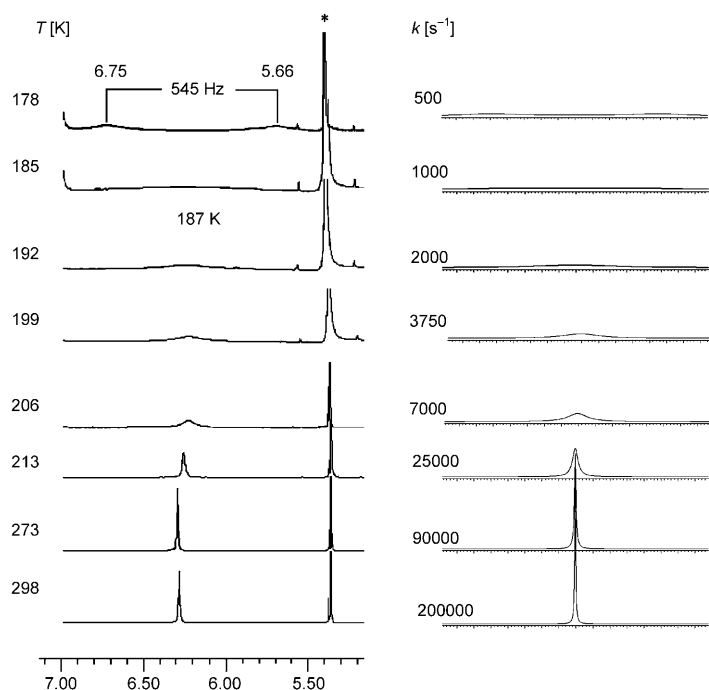

Scheme 2. Triple rotation process.

Figure 4. Left: Experimental temperature dependence of the ^{1}H NMR (500 MHz) methylene proton signals of **6** in CD_2Cl_2. Right: Line-shape simulation obtained with the rate constants indicated.

imprecise and by using the Eyring equation, we have calculated that $\Delta H^{\neq} = 31.6\ \mathrm{kJ\,mol^{-1}}$ and $\Delta S^{\neq} = -12.4\ \mathrm{J\,mol^{-1}\,K^{-1}}$ (6 values: $R^2 = 0.97$) for compound **6**.

Theoretical study: In order to predict conformation preferences, we have calculated the relative energies corresponding to different conformers at the B3LYP/6-31G* level (Table 2).

Table 2. Energy results.

Compound	Configuration[a]	E_{total} [Hartree]	E_{rel} [kJ mol^{-1}]
2	u,u,u, A,A,A	−1898.96585	22.7
	u,u,d, A,A,A	−1898.96865	15.4
	u,u,u, B,B,B	−1898.97451	0.0
	u,u,d, B,B,B	−1898.97156	7.7
3	u,u,u, B,B,B	−2359.90773	2.5
	u,u,d, B,B,B	−2359.90868	0.0
4	u,u,u, B,B,B	−2359.90069	0.0
	u,u,d, B,B,B	−2359.89606	12.1
6	u,u,u, in, B,B,B	−1947.08190	28.0
	u,u,u, out, B,B,B	−1947.09256	0.0
	u,u,d, out, B,B,B	−1947.09070	4.9
	u,u,u, out, A,A,A	−1947.07617	43.0
	u,u,u, out, B,B,A	−1947.09085	4.5
7	u,u,u, in, A,A,A	−1947.07112	28.4
	u,u,d, out, A,A,A	−1947.07468	19.0
	u,u,u, in, B,B,B	−1947.07872	8.4
	u,u,u, out, B,B,B	−1947.08193	0.0

[a] u and d: Position of the aryl rings (up or down). There are only two conformations: $u,u,u \equiv d,d,d$ and $u,u,d \equiv u,d,d$. in and out: Inside or outside position of the N atom. A and B: Relative position of CH_2 and (hetero)aryl groups with respect to the platform (on the same or the opposite side to the triindole).

As a general trend, it has been observed that conformers in which the CH_2 groups of the (hetero)aryl branches are placed below the triindole platform (B,B,B) are the most stable. In all of the studied derivatives (Table 2), except compound **3**, a preference for a conformation with all branches on the same side (u,u,u) has been predicted. For compounds **4** and **6**, there is a perfect agreement between the calculated minimum energy conformation (Table 2) and the determined X-ray structure, whereas, the conformation determined by X-ray crystallography in the case of **3** lies only 2.5 kJ mol^{-1} higher than the most stable conformation calculated.

The experimental barriers appear to be almost independent of the nature of substituent R, so we have calculated the rotation barrier for the simplest compound **2**. To transform the u,u,u,B,B,B minimum into its d,d,d,B,B,B enantiomer, the three R groups must rotate. This process, which permutes the a/b protons of the methylene groups, has the profile represented in Figure 5. The calculated values, including the zero-point energy correction, are TS1 = 31.4 kJ mol^{-1} and TS2 = 38.5 kJ mol^{-1} (for **6**, TS1 = 33.0 kJ mol^{-1}). These values compare very well with the experimental value of 35 ± 2 kJ mol^{-1} (Table 1).
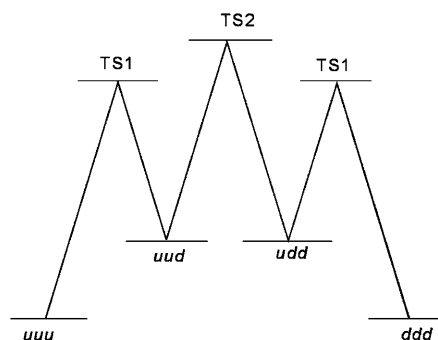

Figure 5. Profile of the triple rotation. TS: transition state.

Conclusion

In conclusion, a new series of *N*-(hetero)arylmethyl triindoles have been synthesized. Theoretical investigations predict a preference for an all-*syn* conformation for these derivatives. Additionally, X-ray analyses confirm that this is the favored conformation in the solid state.

The computational level selected for the present study, B3LYP/6-31G*, is able to reproduce both the minimum energy conformations and the rotation barriers about the N−CH_2 bond. For compounds **4** and **6**, there is a perfect agreement between the calculated minimum energy conformation (Table 2) and the determined X-ray structure, whereas the conformation determined by the X-ray study in the case of **3** lies only 2.5 kJ mol^{-1} higher than the most stable conformation calculated.

The triindole platform offers an electron-rich surface with several unique features, such as ready availability, structural simplicity, and versatility in derivatization. These character-

istics, together with the flexible yet preorganized geometry of trialkylated triindoles, render this platform an attractive candidate in the construction of supramolecular systems.

Experimental Section

General: Routine ¹H and ¹³C NMR spectra were recorded on Bruker AMX 300 and Bruker AC-200 spectrometers. Solvents were purified and dried by using standard procedures. Chromatography purifications were carried out by using flash-grade silica gel with distilled solvents. All reactions were carried out under Ar.

5,10,15-Tribenzyl-10,15-dihydro-5*H*-diindolo[3,2-*a*:3′,2′-*c*]carbazole (2): A mixture of **1** (170 mg, 0.5 mmol), KOH (560 mg, 10 mmol), and [CH₃(CH₂)₃]₄N(HSO₄) (8.5 mg, 0.025 mmol) was heated to reflux in acetone (25 mL). Benzyl bromide (400 μL, 3.36 mmol) was then added and the mixture was stirred for 3 h. The mixture was diluted with EtOAc, washed with 10% aqueous HCl and with saturated aqueous NaCl solution, and dried (Na₂SO₄); the solvent was then evaporated. The residue was triturated with hexanes to give **2** as a white solid (289 mg, 94%). M.p. > 250 °C; ¹H NMR (300 MHz, CDCl₃): δ = 8.00 (d, *J* = 8.1 Hz, 3H), 7.52 (d, *J* = 7.1 Hz, 6H), 7.44 (t, *J* = 7.3 Hz, 6H), 7.39–7.33 (m, 3H), 7.28–7.20 (m, 6H), 7.04–6.99 (m, 3H), 6.09 ppm (s, 6H); ¹³C NMR (50 MHz, CDCl₃): δ = 141.70, 139.62, 138.15, 129.01, 127.37, 126.53, 123.15, 121.51, 120.21, 110.79, 103.23, 51.38 ppm; FAB MS: *m/z* (%): 615 [*M*⁺] (9), 307 (25), 154 (100); HRMS (FAB): calcd for C₄₅H₃₃N₃: 615.2674; found: 615.2683.

5,10,15-Tris(naphthalen-2-ylmethyl)-10,15-dihydro-5*H*-diindolo[3,2-*a*:3′,2′-*c*]carbazole (3): A mixture of **1** (170 mg, 0.5 mmol), KOH (560 mg, 10 mmol), and [CH₃(CH₂)₃]₄N(HSO₄) (8.5 mg, 0.025 mmol) was heated to reflux in acetone (25 mL). 2-(Bromomethyl)naphthalene (718 mg, 3.25 mmol) was added and the mixture was stirred for 3 h. The mixture was diluted with EtOAc, washed with 10% aqueous HCl and with saturated aqueous NaCl solution, and dried (Na₂SO₄); the solvent was then evaporated. The residue was triturated with CH₃CN to give **3** as a white solid (351 mg, 92%). M.p. > 250 °C; ¹H NMR (300 MHz, CDCl₃): δ = 8.05 (d, *J* = 7.6 Hz, 3H), 8.05 (s, 3H), 7.98 (d, *J* = 8.2 Hz, 3H), 7.92 (d, *J* = 8.8 Hz, 3H), 7.77 (d, *J* = 7.1 Hz, 3H), 7.65 (d, *J* = 8.8 Hz, 3H), 7.54–7.45 (m, 6H), 7.28 (d, *J* = 8.2 Hz, 3H), 7.19–7.14 (m, 3H), 6.94 (t, *J* = 7.6 Hz, 3H), 6.26 ppm (s, 6H); ¹³C NMR (75 MHz, CDCl₃): δ = 142.07, 139.90, 135.88, 133.74, 132.93, 129.25, 128.16, 128.02, 126.62, 126.23, 125.62, 124.76, 123.61, 123.42, 121.72, 120.72, 111.23, 103.64, 51.95 ppm; MALDI-TOF MS: *m/z*: 765; HRMS (MALDI-TOF): calcd for C₅₇H₃₉N₃: 765.3138; found: 765.3147.

5,10,15-Tris(naphthalen-1-ylmethyl)-10,15-dihydro-5*H*-diindolo[3,2-*a*:3′,2′-*c*]carbazole (4): A mixture of **1** (170 mg, 0.5 mmol), KOH (560 mg, 10 mmol), and [CH₃(CH₂)₃]₄N(HSO₄) (8.5 mg, 0.025 mmol) was heated to reflux in acetone (25 mL). 1-(Chloromethyl)naphthalene (610 μL, 3.25 mmol) was added and the mixture was stirred for 3 h. The mixture was diluted with EtOAc, washed with 10% aqueous HCl and with saturated aqueous NaCl solution, and dried (Na₂SO₄); the solvent was then evaporated. The residue was triturated with CH₃CN to give **4** as a white solid (321 mg, 84%). M.p. > 250 °C; ¹H NMR (200 MHz, CDCl₃): δ = 8.16–8.11 (m, 3H), 8.08–8.03 (m, 3H), 7.90 (d, *J* = 8.7 Hz, 3H), 7.78 (d, *J* = 8.1 Hz, 3H), 7.69–7.61 (m, 9H), 7.42 (t, *J* = 7.8 Hz, 3H), 7.17–7.04 (m, 6H), 6.65 (t, *J* = 6.7 Hz, 3H), 6.41 ppm (s, 6H); ¹³C NMR (50 MHz, CDCl₃): δ = 141.72, 139.70, 133.86, 133.06, 130.35, 129.12, 128.13, 126.77, 126.16, 126.02, 124.82, 123.18, 122.99, 122.35, 121.43, 120.33, 110.63, 103.42, 49.66 ppm; MALDI-TOF MS: *m/z*: 765; HRMS (MALDI-TOF): calcd for C₅₇H₃₉N₃: 765.3138; found: 765.3149.

5,10,15-Tris(anthracen-9-ylmethyl)-10,15-dihydro-5*H*-diindolo[3,2-*a*:3′,2′-*c*]carbazole (5): A mixture of **1** (102 mg, 0.3 mmol), KOH (336 mg, 6 mmol), and [CH₃(CH₂)₃]₄N(HSO₄) (5.1 mg, 0.015 mmol) was heated to reflux in acetone (25 mL). 9-(Bromomethyl)anthracene (542 mg, 2 mmol) was added and the mixture was stirred for 16 h. The mixture was diluted with Et₂O, washed with 10% aqueous HCl and with saturated aqueous NaCl solution, and dried (Na₂SO₄); the solvent was then evaporated. The residue was triturated with CH₃CN to give **5** as a yellow solid (230 mg,

84%). M.p. > 250 °C; ¹H NMR (300 MHz, C₂D₂Cl₄, 110 °C): δ = 8.43 (d, *J* = 8.1 Hz, 3H), 8.42 (s, 3H), 8.30 (d, *J* = 7.9 Hz, 6H), 7.97 (d, *J* = 7.9 Hz, 6H), 7.39–7.28 (m, 12H), 7.23 (s, 6H), 6.91–6.86 (m, 6H), 6.73 ppm (t, *J* = 7.9 Hz, 3H); MALDI-TOF MS: *m/z*: 915; HRMS (MALDI-TOF): calcd for C₆₉H₄₅N₃: 915.3608; found: 915.3627.

5,10,15-Tris(pyridin-2-ylmethyl)-10,15-dihydro-5*H*-diindolo[3,2-*a*:3′,2′-*c*]carbazole (6): A mixture of **1** (60 mg, 0.173 mmol), KOH (277 mg, 4.97 mmol), and [CH₃(CH₂)₃]₄N(HSO₄) (19.6 mg, 0.058 mmol) was heated to reflux in acetone (9 mL). 2-Picolylchloride hydrochloride (171 mg, 1.04 mmol) was added and the mixture was stirred for 24 h. The mixture was cooled to room temperature and the solvent was evaporated. The mixture was diluted with CH₂Cl₂, washed with water, and dried (Na₂SO₄); the solvent was then evaporated. The residue was triturated with CH₃CN to give **6** as a white solid (54 mg, 50%). M.p. 231–233 °C; ¹H NMR (200 MHz, CDCl₃): δ = 8.82–8.78 (m, 3H), 7.94 (d, *J* = 8.1 Hz, 3H), 7.66–7.58 (m, 3H), 7.32–7.23 (m, 9H), 7.12–7.02 (m, 6H), 6.27 ppm (s, 6H); ¹³C NMR (50 MHz, CDCl₃): δ = 158.43, 149.93, 141.48, 139.34, 137.38, 123.50, 122.97, 122.46, 121.66, 121.45, 120.60, 110.62, 103.54, 53.27 ppm; MALDI-TOF MS: *m/z*: 618 [*M*⁺]; HRMS (MALDI-TOF): calcd for C₄₂H₃₀N₆: 618.25265; found: 618.25146.

5,10,15-Tris(pyridin-3-ylmethyl)-10,15-dihydro-5*H*-diindolo[3,2-*a*:3′,2′-*c*]carbazole (7): A mixture of **1** (60 mg, 0.173 mmol), KOH (280 mg, 5 mmol), and [CH₃(CH₂)₃]₄N(HSO₄) (20 mg, 0.059 mmol) was heated to reflux in acetone (10 mL). 3-Picolylchloride hydrochloride (195 mg, 1.18 mmol) was added and the mixture was stirred for 21 h. The mixture was cooled to room temperature and the solvent was evaporated. The mixture was diluted with CH₂Cl₂, washed with water, and dried (Na₂SO₄); the solvent was then evaporated. The residue was triturated with CH₃CN to give **7** as a white solid (89 mg, 83%). M.p. 280–282 °C; ¹H NMR (200 MHz, CDCl₃): δ = 8.77–8.76 (m, 3H), 8.62–8.59 (m, 3H), 7.92 (d, *J* = 8.0 Hz, 3H), 7.69–7.65 (m, 3H), 7.32–7.23 (m, 9H), 7.14–7.06 (m, 3H), 6.09 ppm (s, 6H); ¹³C NMR (50 MHz, CDCl₃): δ = 148.98, 148.16, 141.55, 139.45, 134.71, 133.72, 124.05, 123.84, 123.28, 121.40, 120.91, 111.01, 103.83, 49.27 ppm; MALDI-TOF MS: *m/z*: 618 [*M*⁺]; HRMS (MALDI-TOF): calcd for C₄₂H₃₀N₆: 618.25265; found: 618.25067.

5,10,15-Tris(pyridin-4-ylmethyl)-10,15-dihydro-5*H*-diindolo[3,2-*a*:3′,2′-*c*]carbazole (8): A mixture of **1** (60 mg, 0.173 mmol), KOH (510 mg, 9 mmol), and [CH₃(CH₂)₃]₄N(HSO₄) (20 mg, 0.059 mmol) was heated to reflux conditions in acetone (10 mL). 4-Picolylchloride hydrochloride (360 mg, 2.19 mmol) was added and the mixture was stirred for 21 h. The mixture was cooled to room temperature and the solvent was evaporated. The mixture was diluted with CH₂Cl₂, washed with water, and dried (Na₂SO₄); the solvent was then evaporated. The residue was triturated with CH₃CN to give **8** as a white solid (72 mg, 67%). M.p. 262–265 °C; ¹H NMR (200 MHz, CDCl₃): δ = 8.71–8.68 (m, 6H), 7.82 (d, *J* = 7.9 Hz, 3H), 7.44–7.41 (m, 6H), 7.33–7.17 (m, 6H), 7.12–7.04 (m, 3H), 6.40 ppm (s, 6H); ¹³C NMR (50 MHz, CDCl₃): δ = 150.54, 147.49, 141.68, 139.42, 123.93, 123.11, 121.71, 121.31, 120.97, 110.84, 103.77, 50.63 ppm; MALDI-TOF MS: *m/z*: 618 [*M*⁺]; HRMS (MALDI-TOF): calcd for C₄₂H₃₀N₆: 618.25265; found: 618.25165.

5,10,15-Tris(quinolin-2-ylmethyl)-10,15-dihydro-5*H*-diindolo[3,2-*a*:3′,2′-*c*]carbazole (9): A mixture of **1** (60 mg, 0.173 mmol), KOH (510 mg, 9 mmol), and [CH₃(CH₂)₃]₄N(HSO₄) (20 mg, 0.059 mmol) was heated to reflux in acetone (10 mL). 2-(Chloromethyl)quinoline hydrochloride (333 mg, 1.55 mmol) was added and the mixture was stirred for 21 h. The mixture was cooled to room temperature and the solvent was evaporated. The mixture was diluted with CH₂Cl₂, washed with water, and dried (Na₂SO₄); the solvent was then evaporated. The residue was triturated with CH₃CN to give **9** as a brown solid (66 mg, 49%). M.p. 248–250 °C; ¹H NMR (200 MHz, CDCl₃): δ = 8.24 (d, *J* = 8.7 Hz, 3H), 8.10–8.04 (m, 6H), 7.87–7.79 (m, 6H), 7.64–7.56 (m, 3H), 7.38–7.27 (m, 6H), 7.22–7.15 (m, 3H), 7.05–6.97 (m, 3H), 6.49 ppm (s, 6H); ¹³C NMR (50 MHz, CDCl₃): δ = 158.94, 148.08, 141.65, 139.53, 137.63, 130.07, 129.08, 127.85, 127.41, 126.61, 123.59, 123.07, 121.75, 120.77, 119.11, 110.93, 103.68, 54.04 ppm; MALDI-TOF MS: *m/z*: 618 [*M*⁺]; HRMS (MALDI-TOF): calcd for C₅₄H₃₆N₆: 768.29960; found: 768.30023.

NMR experiments: Variable-temperature NMR experiments in the range 298–178 K were recorded in CD_2Cl_2 on a Bruker DRX-500 spectrometer operating at 500 MHz (^1H NMR).

X-ray structure determinations

Compound 3: Colorless crystals of **3** showing well-defined faces were mounted on a Bruker Smart CCD diffractometer equipped with a normal-focus, 2.4 kW sealed-tube X-ray source (MoKα radiation, $\lambda = 0.71067$ Å) operating at 50 kV and 20 mA. Data were collected over a hemisphere of the reciprocal space by a combination of three exposure sets. Each exposure of 10 s covered 0.3° in the ω angle over the range $2° < \theta < 28°$. The first 100 frames were recollected at the end of the data collection to monitor crystal decay. The intensities were corrected for Lorentz and polarization effects. The structures were solved by the Multan and Fourier methods. Crystal dimensions: $0.30 \times 0.20 \times 0.20$ mm³; unit-cell dimensions: $a = 15.9573(7)$, $b = 15.9573(7)$, $c = 38.361(2)$ Å; $\gamma = 120(0)°$; $V = 8459.4(7)$ Å³; $Z = 6$; trigonal; $R\bar{3}$ space group; $\rho_{calcd} = 0.902$ mg m⁻³. **3** was refined anisotropically; $R1(F) = 0.0696$ for observed data $(I > 2\sigma(I))$; $R1(F) = 0.1540$ for all data; GOF($F2$) = 0.91.

Compound 4: Colorless crystals of **4** showing well-defined faces were mounted on a Bruker SMART 6 K CCD area-detector three-circle diffractometer with a rotating anode generator (Cu-Kα radiation, $\lambda = 1.54178$ Å) equipped with Goebel mirrors operating at 50 kV and 100 mA. Data were collected over a hemisphere of the reciprocal space by a combination of six exposure sets. Each exposure of 10 s covered 0.3° in the ω angle over the range $3° < \theta < 70°$. The first 100 frames were recollected at the end of the data collection to monitor crystal decay. The intensities were corrected for Lorentz and polarization effects. The structures were solved by the Multan and Fourier methods. Crystal dimensions: $0.20 \times 0.20 \times 0.20$ mm³; unit-cell dimensions: $a = 21.0405(4)$, $b = 16.5374(3)$, $c = 26.5569(5)$ Å; monoclinic; $C2/c$ space group; $\beta = 98.253(1)°$; $V = 9144.9(3)$ Å³; $Z = 8$; $\rho_{calcd} = 1.113$ mg m⁻³. **4** was refined anisotropically; $R1(F) = 0.0752$ for observed data $(I > 2\sigma(I))$; $R1(F) = 0.1138$ for all data; GOF($F2$) = 0.966.

Compound 6: Colorless crystals of **6** showing well-defined faces were mounted on a Bruker Smart CCD diffractometer equipped with a normal-focus, 2.4 kW sealed-tube X-ray source (MoKα radiation, $\lambda = 0.71067$ Å) operating at 50 kV and 30 mA. Data were collected over a hemisphere of the reciprocal space by a combination of three exposure sets. Each exposure of 10 s covered 0.3° in the ω angle over the range $2° < \theta < 26°$. The first 100 frames were recollected at the end of the data collection to monitor crystal decay. The intensities were corrected for Lorentz and polarization effects. The structures were solved by the Multan and Fourier methods. Crystal dimensions: $0.46 \times 0.18 \times 0.18$ mm³; unit-cell dimensions: $a = 22.7626(8)$, $b = 22.7626(8)$, $c = 10.7613(5)$ Å; $\gamma = 120(0)°$; $V = 4828.8(3)$ Å³; $Z = 3$; trigonal; $P3$ space group; $\rho_{calcd} = 1.364$ mg m⁻³. **6** was refined anisotropically; $R1(F) = 0.091$ for observed data $(I > 2\sigma(I))$; $R1(F) = 0.133$ for all data; GOF($F2$) = 1.07.

Although this structure is apparently centrosymmetric ($P\bar{3}$ space group), the guest molecules break the symmetry of the inversion center. Therefore, the structure was solved and refined in $P3$ group.

Most of the calculations were carried out with SMART[15] software for data collection and reduction and with SHELXTL[16] software for structure solutions and refinements of **3**, **4**, and **6**. CCDC 633826 (**3**), 633827 (**4**), and 687516 (**6**) contain the supplementary crystallographic data for this paper. These data can be obtained free of charge from the Cambridge Crystallographic Data Centre via www.ccdc.cam.ac.uk/data_request/cif. The solvent molecules in **3** and **4** could not be modeled properly and have been disregarded. The SQUEEZE[17] program was used to calculate the solvent disorder area and remove its contribution to the overall intensity data. The calculated density for **3** is lower than 1.0 mg m⁻³ because of this.

Computational Details

Optimizations of geometries of the structures were carried out at the B3LYP/6-31G*[18–21] within the Gaussian 03 package.[22] The transition states were located by the synchronous transit-guided quasi-Newton (STQN) method by using the QST2 keyword.[23] Frequency calculations at the same computational level were carried out to confirm that the obtained structures correspond to energy minima or transition states. GIAO absolute shieldings[24,25] were calculated on the B3LYP/6-311++G** optimized geometries.

[1] a) C. Moberg, *Angew. Chem.* **1998**, *110*, 260–281; *Angew. Chem. Int. Ed.* **1998**, *37*, 248–268; b) C. Moberg, *Angew. Chem.* **2006**, *118*, 4838–4840; *Angew. Chem. Int. Ed.* **2006**, *45*, 4721–4723.

[2] Preorganization of hexasubstituted benzenes has been known for a long time: a) D. J. Iverson, G. Hunter, J. F. Blount, J. R. Damewood, K. Mislow, *J. Am. Chem. Soc.* **1981**, *103*, 6073–6083; b) D. D. MacNicol, A. D. U. Hardy, D. R. Wilson, *Nature* **1977**, *266*, 611–612.

[3] a) D. R. Turner, M. J. Paterson, J. W. Steed, *J. Org. Chem.* **2006**, *71*, 1598–1608; b) H. Abe, Y. Aoyagi, M. Inouye, *Org. Lett.* **2005**, *7*, 59–61. For reviews on the use of preorganized persubstituted benzenes in host–guest chemistry, see: c) S. L. Wiskur, H. Aït-Haddou, J. J. Lavigne, E. Anslyn, *Acc. Chem. Res.* **2001**, *34*, 963–972; d) G. Hennrich, E. Anslyn, *Chem. Eur. J.* **2002**, *8*, 2219–2223.

[4] a) S. R. Waldvogel, R. Fröhlich, C. A. Schalley, *Angew. Chem.* **2000**, *112*, 2580–2583; *Angew. Chem. Int. Ed.* **2000**, *39*, 2472–2475; b) H.-J. Choi, Y. S. Park, S. H. Yun, H.-S. Kim, C. S. Cho, K. Ko, K. H. Ahn, *Org. Lett.* **2002**, *4*, 795–798; c) R. A. Pascal, Jr., M. S. Mathai, X. Shen, D. M. Ho, *Angew. Chem.* **2001**, *113*, 4882–4884; *Angew. Chem. Int. Ed.* **2001**, *40*, 4746–4748.

[5] a) M. J. Plater, *J. Chem. Soc. Perkin Trans. 1* **1997**, 2897–2901; b) B. Gómez-Lor, C. Koper, R. H. Fokkens, E. J. Vlietstra, T. J. Cleij, L. W. Jenneskens, N. M. M. Nibbering, A. M. Echavarren, *Chem. Commun.* **2002**, 370–371; c) B. Gómez-Lor, E. González-Cantalapiedra, M. Ruiz, O. de Frutos, D. J. Cárdenas, A. Santos, A. M. Echavarren, *Chem. Eur. J.* **2004**, *10*, 2601–2608.

[6] a) E. M. Pérez, M. Sierra, L. Sánchez, M. R. Torres, R. Viruela, P. M. Viruela, E. Ortí, N. Martín, *Angew. Chem. Int. Ed.* **2007**, *46*, 847–1851; b) Ó. de Frutos, B. Gómez-Lor, T. Granier, Á. Monge, E. Gutiérrez-Puebla, A. M. Echavarren, *Angew. Chem.* **1999**, *111*, 186–189; *Angew. Chem. Int. Ed.* **1999**, *38*, 204–207; c) B. Gómez-Lor, Ó. de Frutos, P. A. Ceballos, T. Granier, A. M. Echavarren, *Eur. J. Org. Chem.* **2001**, 2107–2114; d) E. González-Cantalapiedra, M. Ruiz, B. Gómez-Lor, B. Alonso, D. García-Cuadrado, D. J. Cárdenas, A. M. Echavarren, *Eur. J. Org. Chem.* **2005**, 4127–4140.

[7] a) Y. Sun, K. Xiao, Y. Liu, J. Wang, J. Pei, D. Zhu, *Adv. Funct. Mater.* **2005**, *15*, 818–822; b) J. Pei, J.-L. Wang, X.-Y. Cao, X.-H. Zhou, W.-B. Zhang, *J. Am. Chem. Soc.* **2003**, *125*, 9944–9945.

[8] a) T. S. Perova, J. K. Vij, *Adv. Mater.* **1995**, *7*, 919–922; b) T. W. Warmerdam, R. J. M. Nolte, W. Drenth, J. C. Van Miltenburg, D. Frenkel, R. J. J. Zijlstra, *Liquid Cryst.* **1988**, *3*, 1087–1104; c) D. Sandström, M. Nygren, H. Zimmermann, A. Maliniak, *J. Phys. Chem.* **1995**, *99*, 6661–6669.

[9] a) B. Gómez-Lor, G. Hennrich, B. Alonso, A. Monge, E. Gutiérrez-Puebla, A. M. Echavarren, *Angew. Chem.* **2006**, *118*, 4603–4606; *Angew. Chem. Int. Ed.* **2006**, *45*, 4491–4494; b) B. Gómez-Lor, B. Alonso, A. Omenat, J. L. Serrano, *Chem. Commun.* **2006**, 5012–5014; c) W.-Y. Lai, Q.-Y. He, R. Zhu, Q.-Q. Chen, W. Huang, *Adv.*

Funct. Mater. **2008**, *18*, 265–276; d) H. Hiyoshi, H. Kumagai, H. OOi, T. Sonoda, S. Mataka, *Heterocycles* **2007**, *72*, 231–238.

[10] N. Robertson, S. Parsons, E. J. MacLean, R. A. Coxall, R. A. Mount, *J. Mater. Chem.* **2000**, *10*, 2043–2047.

[11] B. Gómez-Lor, A. M. Echavarren, *Org. Lett.* **2004**, *6*, 2993–2996.

[12] The conformation of these systems has been described by using the following nomenclature: *u* and *d*: up and down of the (hetero)aryl ring (there are only two conformations: *u,u,u ≡ d,d,d* and *u,u,d ≡ u,d,d*); *in* and *out* in the case of heterocycles: inside or outside position of the N atom; *A* and *B*: relative position of CH_2 and (hetero)-aryl groups with respect to the platform (on the same side as or the opposite side to the triindole).

[13] J. Elguero, C. Marzin, D. Tizané, *Org. Magn. Reson.* **1969**, *1*, 249–275.

[14] P. H. M. Budzelaar, gNMR, Ver. 5.0 IvorySoft, Cherwell Scientific, Oxford, UK, **2004**.

[15] Software for the SMART system, Ver. 5.04, Bruker–Siemens Analytical X-ray Instruments, Inc., Madison, WI, **1998**.

[16] G. M. Sheldrick, SHELXL97, Program for Crystal Structure Refinement, University of Göttingen, Germany, **1997**.

[17] A. L. Spek, PLATON, A Multipurpose Crystallographic Tool, Utrecht University, Utrecht, The Netherlands, **2005**.

[18] A. D. Becke, *Phys. Rev. A* **1988**, *38*, 3098–3100.

[19] A. D. Becke, *J. Chem. Phys.* **1993**, *98*, 5648–5652.

[20] C. Lee, W. Yang, R. G. Parr, *Phys. Rev. B* **1988**, *37*, 785–789.

[21] P. A. Hariharan, J. A. Pople, *Theor. Chim. Acta* **1973**, *28*, 213–222.

[22] Gaussian 03, M. J. Frisch, G. W. Trucks, H. B. Schlegel, G. E. Scuseria, M. A. Robb, J. R. Cheeseman, J. A. Montgomery, Jr., T. Vreven, K. N. Kudin, J. C. Burant, J. M. Millam, S. S. Iyengar, J. Tomasi, V. Barone, B. Mennucci, M. Cossi, G. Scalmani, N. Rega, G. A. Petersson, H. Nakatsuji, M. Hada, M. Ehara, K. Toyota, R. Fukuda, J. Hasegawa, M. Ishida, T. Nakajima, Y. Honda, O. Kitao, H. Nakai, M. Klene, X. Li, J. E. Knox, H. P. Hratchian, J. B. Cross, C. Adamo, J. Jaramillo, R. Gomperts, R. E. Stratmann, O. Yazyev, A. J. Austin, R. Cammi, C. Pomelli, J. W. Ochterski, P. Y. Ayala, K. Morokuma, G. A. Voth, P. Salvador, J. J. Dannenberg, V. G. Zakrzewski, S. Dapprich, A. D. Daniels, M. C. Strain, O. Farkas, D. K. Malick, A. D. Rabuck, K. Raghavachari, J. B. Foresman, J. V. Ortiz, Q. Cui, A. G. Baboul, S. Clifford, J. Cioslowski, B. B. Stefanov, G. Liu, A. Liashenko, P. Piskorz, I. Komaromi, R. L. Martin, D. J. Fox, T. Keith, M. A. Al-Laham, C. Y. Peng, A. Nanayakkara, M. Challacombe, P. M. W. Gill, B. Johnson, W. Chen, M. W. Wong, C. Gonzalez, J. A. Pople, Gaussian, Inc., Pittsburgh, PA, **2003**.

[23] C. González, H. B. Schlegel, *J. Chem. Phys.* **1989**, *90*, 2154–2161.

[24] R. Ditchfield, *Mol. Phys.* **1974**, *27*, 789–807.

[25] F. London, *J. Phys. Radium* **1937**, *8*, 397–409.